THE INTERNATIONAL JOURNAL OF SCIENCE & TECHNOLEDGE

Effect of Fiber Draw Ratio and Fiber Weight Fraction on Creep, Fatigue and Dynamic Mechanical Behaviour of Self-Reinforced Polypropylene Composite

Wanyama Paul Simiyu
School of Pure and Applied Sciences, Department of Physics, Kenyatta University, GPO, Nairobi, Kenya.
Migwi Charles Maina
School of Pure and Applied Sciences, Department of Physics, Kenyatta University, GPO, Nairobi, Kenya.
Barasa Daniel Bem
School of Pure and Applied Sciences, Department of Physics, Kenyatta University, GPO, Nairobi, Kenya.

Abstract:
The creep, fatigue and dynamic mechanical behaviour of the SRPPCs was studied by using TA Instruments DMA 2980 machine. Dynamic mechanical analysis was done in the temperature range 30 to 110^oC at 1Hz using the single cantilever flexural mode. The test was carried out at in the amplitude controlled single frequency mode at 5Hz, stress ratio(R=1), temperature 35^oC and 140 minutes experimental time. Fiber draw ratios of 2, 5, 8, and 11were used for the Dr Sample category, while fiber weight fractions of 3, 6, 9, and 12were selected. The incorporation of drawn polypropylene fibers improved the stiffness and fatigue resistance of the self-reinforced composite especially at high draw ratio (11) and high fiber weight fraction (12). Good correlation was found between both fiber draw ratio and fiber weight fraction with mechanical properties of the composite. Short-term isothermal creep tests were carried out using single cantilever tensile mode on the two sample categories at different temperatures ranging from 30 to 90^oC under an applied stress of 5MPa. Remarkable improvement on creep resistance occurred when fiber draw ratio and fiber weight fraction were maintained at 11 and 15wt% respectively. Burger's models could satisfactorily be applied to analyse the short-term creep behaviour of the composites. Creep master curves were created using time-temperature superposition principle (TTSP). Using the master curves, creep deformation of order 10^8 minutes could be predicted. The temperature dependence of the shift factors could best be described by the Arrhenius equation. All these positive gains made in mechanical properties are attributed to fiber drawing which enhances molecular orientation (crystalline regions) and minimizes segmental movement of the chain molecules.

Keywords: *reinforcements, self-reinforced composites, fatigue, SRPPC, PP, Mechanical properties, recyclability.*

1. Introduction

Self–reinforced polypropylene composites have tremendous growth potential in commercial, military, automotive, aerospace and structural applications as well as numerous applications which all require light weight, high performance materials [2–7]. Moreover, the overall ease of recyclability of self-reinforced polypropylene composites makes such materials attractive. This enhanced recyclability is necessary to fulfil environmental legislations focusing on industries such as automotive industry [1].

In many applications of polymer composite materials loading is usually static or cyclic in nature. Sometimes the application environments of these materials is also extremely harsh and hostile, which means that tests on effects of these conditions on the mechanical properties of self-reinforced polymer composites are vital.

Former researchers have shown that the creep behaviour of self-reinforced polypropylene composites depends mainly on stress, temperature, void content, and fibre loading [8–10]. Their findings reveal that, creep resistance decreases if temperature or stress rises. Numerous other studies exploredhow interfacial strength and density of the composites influence the creep behaviour [11–13]. And, the results show that with increasing consolidation (lower void content) the resistance to creep increases.

On the impact performance, the self-reinforced polypropylene composites possess excellent resistance to falling weight impact penetration and can compete or outperform glass or natural fiber reinforced polypropylene composites [14]. Impact performance increases with decreasing interfacial strength, with penetrating energy increasing with decreasing compaction temperature and pressure. Since the interfacial strength is controlled by processing conditions, it is possible to tailor the impact resistance by altering tape production parameters or composite compaction parameters [14].

The physical properties of polymeric materials are strongly dependent on morphology, structure and relaxation processes corresponding to internal changes and molecular motions. Dynamic mechanical measurements over a wide temperature or

frequency ranges provide valuable insights into the relationship between structure, morphology and properties of polymers and polymer composites. Structure-property relationships in self-reinforced PP composites were disclosed based on dynamic mechanical thermal analysis of all-PP composite laminates with unidirectional (UD) and cross-ply (CP) lay-ups. The results showed that all-PP composites with UD lay-ups were stiffer resulting from higher crystallinity (revealed by higher enthalpy of fusion) in the specimens. Furthermore, DMA investigations displayed no significant glass transition for the all-PP tapes and their composites due to the high degree of crystallinity and molecular orientation in the all-PP tapes. However, fatigue behaviour was less considered for all-PP composites.
The aim of this study was to investigate the effect of fiber draw ratio and fiber weight fraction on creep, fatigue and dynamic mechanical behaviour of self-reinforced polypropylene composite.

2. Experimental

2.1. Materials

Commercial isotactic homopolymer polypropylene in the form of round milky pellets of average diameter 3 mm, obtained from General Plastics Nairobi Kenya, was used in this study.

2.2. Composite Preparation

Specimen were produced by compression moulding using film stacking technique. The reinforcing fibers were drawn at room temperature of 25^{o}C at a rate of 7.2 revolutions per minute. Self-reinforced PP composite (SRPPC) measuring 34mm by 12mm by 2.5mm were fabricated. The reinforcement content in the samples ranged between 3 to 15wt%, while the draw ratio was in the ranged2 to 11. The samples were consolidated at 170^{o}C, while the processing time was maintained at 130 seconds, and pressure held at 40N.

2.3. Testing

2.3.1. Dynamic Mechanical Analysis of SRPPC

DMA of self-reinforced PP composites was performed in single cantilever flexural mode. Specimens with dimensions of approximately 35mm x 12mm x 2.5mm (standard specimen dimensions for the DMA test) were tested in the DMA 2980 machine (TA Instruments) equipped with a data acquisition software. After loading the specimens the temperature was raised to 35^{o}C and allowed to stabilize. After equilibration, the chamber was heated at a rate of 2^{o}C per minute until 110^{o}C. The specimen was subjected to a sinusoidal flexural displacement applying a maximum tensile strain of 0.04 % at frequency of 1Hz. This test was carried out on all the five categories of samples prepared. The damping factor tanδ, storage and loss moduli were monitored and recorded as functions of temperature, draw ratio and fiber weight fraction.

2.3.2. Fatigue Test

The fatigue behaviour of the SRPPCs was studied by using TA Instruments DMA 2980 machine. The DMA single frequency mode was selected. Fatigue tests were conducted in an amplitude controlled mode at a frequency of 5 Hz and stress ratio (R=1). A cyclic frequency of 5 Hz was used to prevent increase in temperature due to hysteretic heating. Such a low frequency was selected so that fatigue failure would occur instead of thermal failure. The duration of fatigue test was 140 minutes. The temperature of the experiment was kept constant at 35ºC and the specimens were tested at 0.04% strain. Fatigue data for all the five sample categories were used to generate stiffness (storage) modulus versus number of cycles (E'–N) curves which were used to characterize fatigue behaviour of the composite.

2.3.3. Creep Test

Short-term flexural creep tests were performed using single cantilever tensile mode at different temperatures, ranging from 30^{o}C to 90^{o}C, in the DMA 2980 apparatus (TA Instruments). In this temperature range, isothermal creep tests were run on the specimens with a stepwise temperature increment of 15^{o}C. Prior to the creep measurement, each specimen was equilibrated for 5 minutes at each temperature and then the tensile creep behaviour was tested for 12 minutes, under a constant stress of 5 MPa. Specimens of dimensions approximately 18mm x 13mm x 2.5mm (length x width x thickness) were used for creep tests. This procedure was applied for all the five categories of samples prepared. The data collected was then used for analysis of creep deformation behaviour of SRPPC.

3. Results and Discussion

3.1. Dynamic Mechanical Analysis of SRPPCS Produced with Polypropylenefibers of Different Draw Ratios

Figure 1 shows a plot of storage modulus E' against temperature for samples produced with fibers of draw ratios 2, 5, 8, 11 and the neat sample. The figure shows that the storage modulus E', for SRPPCs increases with fiber draw ratio at a specific temperature. Neat PP has the lowest storage modulus compared to reinforced samples. This observation emphasises the reinforcing effectiveness of the drawn PP fibers.

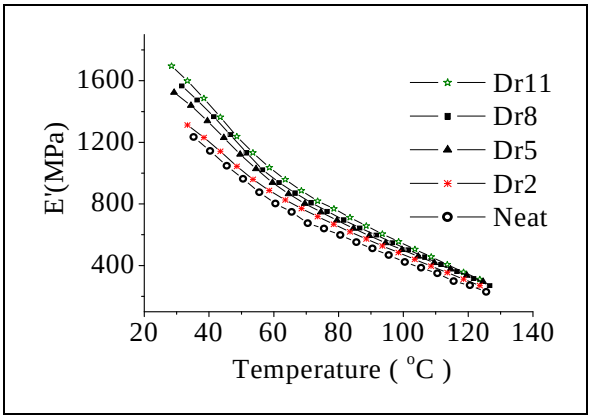

Figure 1: Storage modulus versus temperaturefor samples produced with fibers of different draw ratios

High values for E', correspond to high degree of orientation of the fibers which restricts segments of chain molecules from moving during deformation. Thus, high draw ratios cause an increase in stiffness of SRPPCs due to increased intermolecular forces. The temperature effect is as expected.

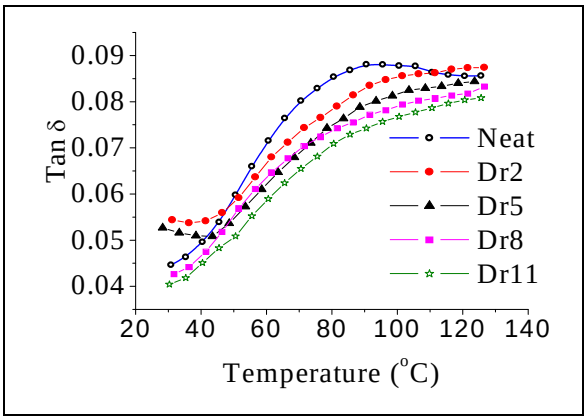

Figure 2: Plots of tan delta againsttemperature for samples produced with fibers of different draw ratios

The influence of fiber draw ratio on the loss factor (tan δ) is shown in figure 2. From the results, it is evident that neat PP has the highest tan delta peak with the highest magnitude (0.0881) at temperature T = 90°C. The peak values for tan delta for other samples decrease gradually with increase in draw ratio. The peaks also shift to higher temperatures. The specimen with fibers of draw ratio 11 has the lowest peak at the highest temperature (tan delta 0.0810 at 120°C).
The observed tan delta peaks above 90°C correspond to α transition (T_α), and are believed to be the result of molecular motions which resist the softening effect of the applied heat. Thus, the onset of segmental motions within the crystalline regions is shifted to higher temperatures due to high orientation of the chain segments as a result of drawing. This implies that high draw ratios are preferred and hence they are highly recommended for fabrication of SRPPCs.

3.2. Effect of Fiber Draw Ratio on Fatigue Behaviour of SRPPCS
Figures 3 shows the effects of different fiber draw ratios on the stiffness of the SRPPCs when subjected to cyclic fatigue. At fatigue strain amplitude of 20μm the specimen achieved 42000 stress cycles and retained high residual storage modulus with respect to the initial value at zero stress cycles. The results also show consistency with DMA results in the sense that the fatigue resistance increases with fiber draw ratio. The sample with the highest draw ratio (Dr11) registered the highest residual storage modulus due to the fact that it is stiffer, thus exhibits more elastic response.

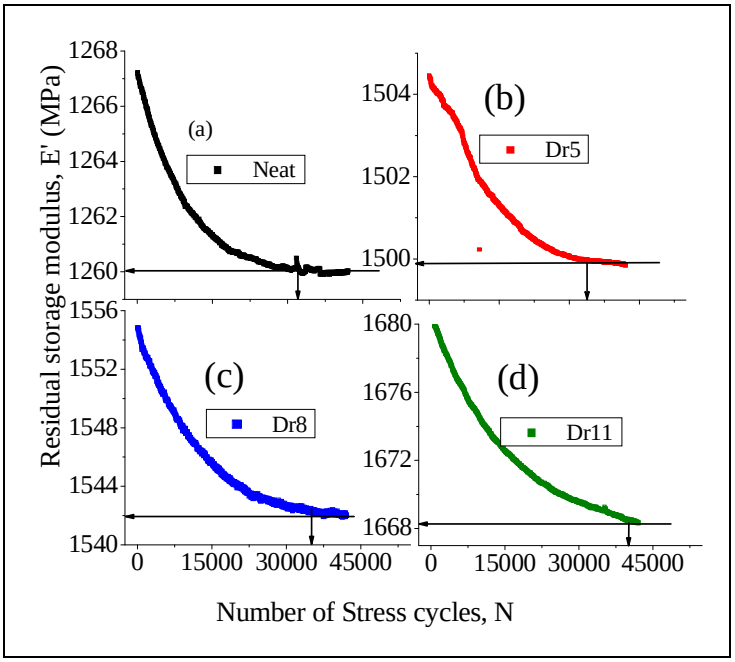

Figure 3: Comparison of fatigue behaviour of neat PP (a) and SRPPCs reinforced with PP fibers of draw ratios, (b) 5, (c) 8 and, (d) 11

On the other hand, the neat sample showed the lowest residual storage modulus after 42000 stress cycles compared to the reinforced specimens. This indicates that samples with lower draw ratios are more flexible. Figures 3 also depict the fatigue resistance and endurance limits of neat, Dr5, Dr8 and Dr11 samples. The fatigue endurance limits for the specimens were exhibited at 31900 (neat), 33800 (Dr5), and 35700 (Dr8) cycles. Specimen Dr11 registered both fatigue resistance and endurance limit of highest magnitudes (1.668GPa and 43400). This sample is stiffer, and thus exhibits more elastic response.

These results clearly indicate that, the storage moduli for all specimens decreased compared to the initial values, after fatigue life of 42000 cycles. However, these changes were small (< 0.01 GPa). In general the modulus for sample Dr11 remained high throughout the fatigue life. The composites retained high moduli values due to induced crystallinity resulting from highly oriented chain molecules that could resist segmental motions due to mechanical cycling. Also, the 5Hz frequency could not allow the chain molecules enough time to respond. Thus, high draw ratios enhance the fatigue resistance and fatigue endurance for SRPPCs. The entire specimen category exhibited a stiffness limit (E' value) below which fatigue failure would be imminent. This limit can be relied on when designing SRPPCs against fatigue failure.

3.3. Effect of Fiber Draw Ratio on Creep Strain of SRPPCS

Samples reinforced with PP fibers of draw ratios Dr2, Dr5, Dr8 and Dr11 were subjected to a constant stress of 5MPa, for 12 minutes at a constant temperature of 35°C (temperature at which materials are used in the tropical areas). Fiber weight fraction, consolidation time and consolidation temperature were kept at 15wt%, 130 seconds and 170°C respectively. Consolidation pressure was maintained at 6MPa. The data obtained were used to plot curves of creep compliance against time as shown in figure 4. The results reveal that, creep strain decreases with increase in fiber draw ratio. Samples reinforced with fibers of draw ratio of 11 exhibited the lowest creep strain. High creep strain implies that the sample is more flexible, while low creep strain signifies resistance to creep deformation. Consequently, creep resistance was seen to increase with fiber draw ratio (Figure 4). Resistance to creep is as a result of higher percentage of crystalline fraction. Drawing increases the orientation of the amorphous regionswhich are confined within the crystalline zones.

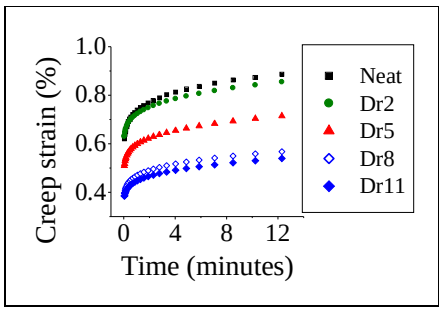

Figure 4: Creep strain versus time for Dr sample category

Thus, drawing prevents mobility of macromolecular chain segments leading to lower deformation of the composites. The drawing process stretches and straightens the polymer chain molecules. The already oriented molecules resist further stretching during creep deformation. Hence, drawing enhances creep resistance of SRPPCs.

3.4. Dynamic Mechanical Analysis of SRPPCS Having Different Fiber Weight Fractions

Weight fraction (wt%) was the varied parameter during investigation of the influence of fiber weight fraction on mechanical properties. Consolidation temperature, consolidation time and fiber draw ratio were kept constant at 170^{o}C, 130 seconds and draw ratio 11 respectively. The different fiber weight fractions used were 3 wt%, 6 wt%, 9 wt%, 12 wt%, and 15 wt%.

The effect of temperature on the dynamic storage modulus and loss factor (tan delta) of the fiber weight fraction (Fw) specimens is shown in figures 5 and 6 respectively. The storage moduli of the composites clearly decreases with increasing temperature as expected in a polymer system. The moduli also increase with fiber weight fraction at a specific temperature value. The effect of fiber weight fraction on storage modulus is more pronounced at low temperatures compared to high temperatures. High initial values of the storage modulus correspond to increased percentage of oriented fibers. A maximum value of 1806 MPa is attained as initial modulus (for Fw = 15%, figure 5).

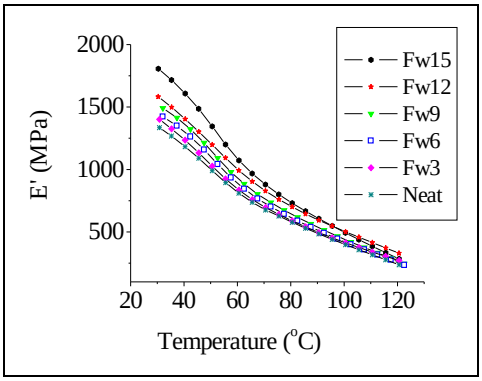

Figure 5: Plots of storage modulus against temperature for samples produced with different fiber weight fractions

From the graph, the curves indicate a clear trend of increasing modulus with fiber weight fraction, corresponding to increasing percentage of oriented regions. Thus, it is clear from this results that the stiffness of the composite is highly dependent on fiber weight fraction (measured by the storage modulus).

Generally the peaks of loss factor (tan delta) are associated with the glass transition temperature T_g (relaxation) at lower temperatures and α transition temperature T_α at higher temperatures. T_g indicates mobility within the amorphous regions, whereas T_α represents the onset of segmental motion within the crystalline regions [16-18]. PP is an "alpha mobile" polymer and therefore exhibits α transition at high temperatures.

In figure 6, the specimens are seen to present tan delta peaks between 85 and 125^{o}C. It is clear that peaks for the reinforced samples are shifted towards higher temperatures and their magnitude is reduced when compared with neat PP. These observations are a result of the amorphous phase in the oriented fibers becoming highly oriented between crystalline regions [6]. The oriented amorphous phase forms taut tie molecules, which restrict molecular segmental mobility. Therefore, the magnitude of the loss factor peaks is reduced and the temperature at which molecular motion is initiated is raised. The tan delta peak of Fw15, although not completely developed seems to be shifted to higher temperature values by more than 25.5^{o}C higher than that for neat PP, demonstrating the improved thermal stability of Fw15 composite.

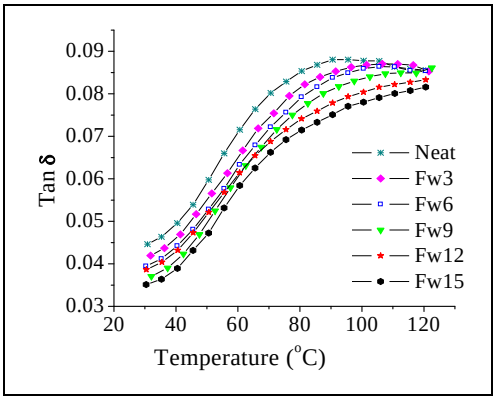

Figure 6: Variation of tan δ with fiber weight fraction

3.5. Effect of Fiber Weight Fraction on Fatigue Behaviour of SRPPCS

The fatigue life times of samples with fiber weight fractions 3, 6, 9, and 12 are shown in figure 7. These results indicate that Fw15 specimen with the highest fiber weight fraction has the greatest residual modulus at the end of fatigue life (42000 cycles).
This can be attributed to the fact that samples with higher fiber weight fraction contain high crystalline structures, thus exhibiting more elastic response.

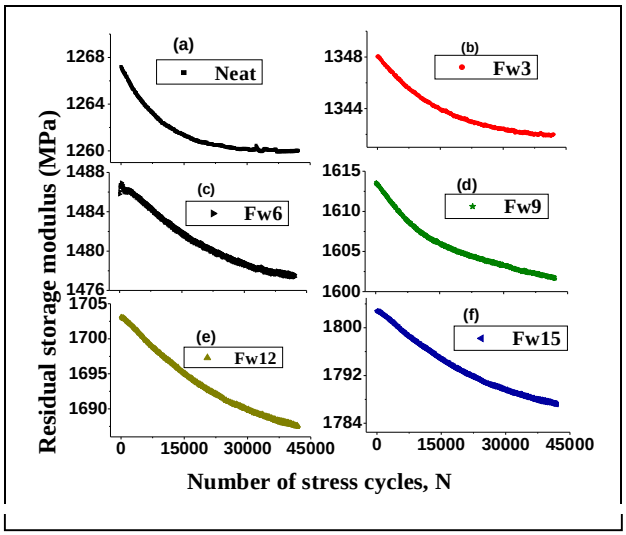

Figure 7: Plots of residual modulus versus number of stress cycles for samples produced with fiber weight fractions: neat (a), Fw3 (b), Fw6 (c), Fw9 (d), Fw12 (e) and Fw15(f)

3.6. Effect of Fiber Weight Fraction on Creep Strain of SRPPCS

The effect of PP fiber weight fraction on the creep strain of the SRPPC is shown in figure 8. From the results the percentage creep strain was observed to decrease with increasing fiber weight fraction. High fiber weight fraction leads to an increase in the oriented and crystalline regions which offer high resistance to polymer chain molecules segmental motion.

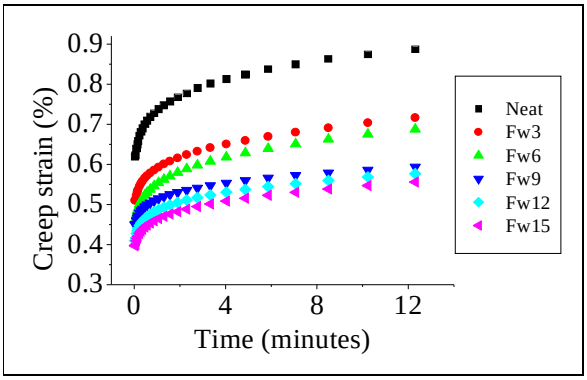

Figure 8: Variation of creep strain with time for the Fw sample category.

Table 1contains creep strain values extracted from figure 8, at the end of 12 minutes during creep deformation. These values were plotted against fiber weight fraction as shown in figure 9.
The results indicate that creep strain decreases gradually with increasing fiber loading. Thus, fiber weight fraction plays a significant role in determining the stiffness of SRPPCs.

Fw	Creep strain (%) at 12 minutes
0	0.88715
3	0.71619
6	0.68775
9	0.59352
12	0.57677
15	0.55612

Table 1: Variation of creep strain with Fiber weight fraction (Fw)

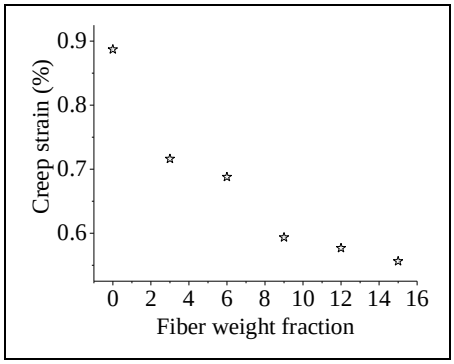

Figure 9: Plot of creep strain versus fiber weight fraction

4. Analysis

4.1. Creep Modelling

Besides experimental observations, creep modelling can be applied to polymeric materials to develop comprehensive understanding of the creep deformation phenomena. In the past half century, numerous creep models have been proposed and applied to describe the creep behaviour of viscoelastic materials [19-21]. The creep-recovery curve can be looked at as a combination of springs (elastic sections) and dashpots (viscous sections). The qualitative form of the basic constitutive equation for creep models is:

$$\varepsilon = \varepsilon_o + \varepsilon_c \quad (1)$$

whereε is the total strain at some time, *t*, after a stress application, ε_c, time-dependent creep component of strain at *t*, and ε_o is the instantaneous strain after stress application. The instantaneous strain component (ε_o) is elastic and the creep component, ε_c, is a simple arithmetic function of time (linear, logarithm, exponential, power law), either alone or in combination.

4.1.1. Burger's Model

The Burger's model is one of the most widely used models. It gives the relationship between the morphology of the composites and their creep behaviour [19, 22, 26]. Burgers model consists of Maxwell and Voigt-Kelvin units combined in series. Figures10show a scheme of the four-element Burger model while figure 11 shows the curve which results from the model. The curve shows the same regions as seen in real materials, including a small instantaneous region, a levelling off of the equilibrium region, and a realistic recovery curve.

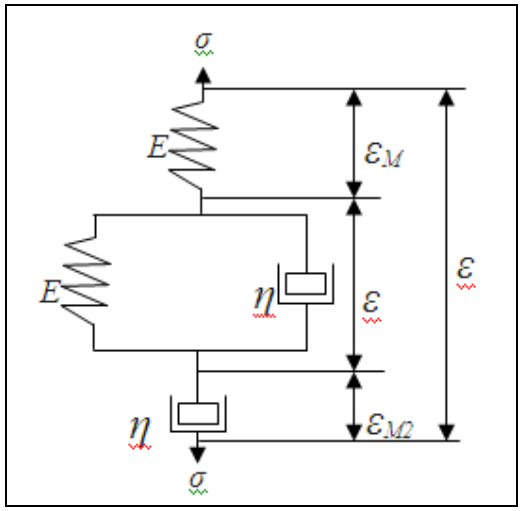

Figure 10: Schematic diagram of Burger's model, [22, and 24]

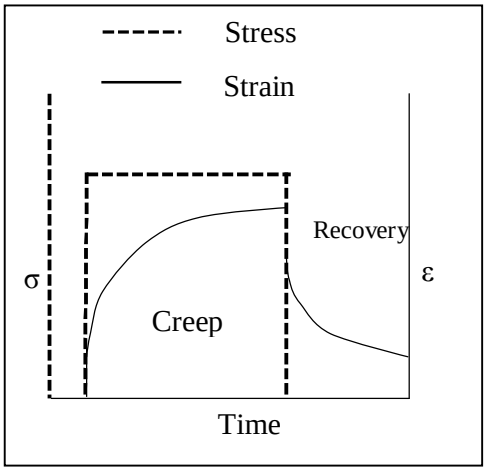

Figure 11: Schematic diagram of Burger's model strain curve [22, 24]

The constitutive equation for a Burger's model can be derived by considering the strain response under constant stress of each coupled element in series as depicted in figure 10. The total strain ε_B at time t is the sum of the strains in these three units, where the spring and dashpot in the Maxwell model are considered as two elements [17, 23], thus:

$$\varepsilon_B = \varepsilon_{M1} + \varepsilon_{M2} + \varepsilon_K \quad (2)$$

Which yields;

$$\varepsilon_B = \frac{\sigma_o}{E_M} + \frac{\sigma_o}{E_K}\left(1 - e^{\frac{-t\eta_K}{E_K}}\right) + \frac{\sigma_o t}{\eta_M} \quad (3)$$

The first term in equation (3.16) is constant and describes the instantaneous elastic deformation; the second one is delayed elasticity of the Kelvin unit and is dominant in the earliest stage of creep, but soon goes to a saturation value close to $\frac{\sigma_o}{E_K}$ (when t $\rightarrow \infty$, $\left(e^{\frac{-t\eta_K}{E_K}}\right) \rightarrow 0$); the viscous flow then increases nearly linearly in the third term after a sufficient long time period of loading. The Burgers model, which includes the essential elements, can be applied satisfactorily to model the practical behaviours of viscoelastic materials. The material parameters E_M, η_M, E_K and η_K can be simulated from the experimental data [19, 25, 26].

The derivative of equation (3) is the creep rate $\left(\dot{\varepsilon}_B\right)$ of the Burgers model,

$$\dot{\varepsilon}_B = \frac{\sigma_o}{\eta_M} + \frac{\sigma_o}{\eta_K} e^{-t\frac{\eta_K}{E_K}} \quad (4)$$

At sufficient long time scale, the creep rate reaches asymptotically to a constant value;

$$\dot{\varepsilon}_B = \frac{\sigma_o}{\eta_M} \quad (5)$$

[19, 25, 26].

4.1.2. Modelling Parameters of Burger's Model And Structure-Property Relationship

The process of determining the initial values of the Burger's model involved first, separating the creep curve into elastic (O-A), viscous (A-B) and viscoelastic (B-C) components as illustrated in figure 12.

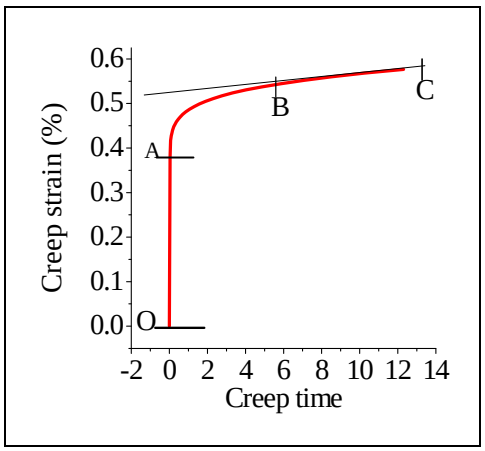

Figure 12: Analysis of creep curve for FW12wt%

The initial values for the Burger's model parameters calculated using figure 12 were; retardation time, τ = 0.364 minutes, modulus of the Maxwell spring, E_M = 23.16, the modulus of the Kelvin spring, E_K=15.57, viscosity of the Maxwell dashpot, η_M= 1720 andthe viscosity of the Kelvin dashpot η_K= 15.

The height of section OA of the curve represents the initial instantaneous strain of the material and is equivalent to $\frac{\sigma_o}{E_M}$. From a molecular perspective this can be viewed as the elastic deformation of the polymer chains. The independent dashpots contribution, η_M, was determined by calculating the slope of the strain curve in the region of viscous equilibrium flow BC. This equilibrium slope is equivalent to $\frac{\sigma_o}{\eta_M}$. The curved region AB is described by the Voigt-Kelvin element of the Burger's model $\frac{\sigma_o}{E_M}\left(1-e^{-t\left(\frac{\eta_K}{E_K}\right)}\right)$ in which $\frac{\eta_K}{E_K}=\tau$ is the retardation time taken to produce 63.2% or (1-e^{-1}) of the total deformation of the Kelvin unit. Molecularly the dashpot in this unit can be considered to represent the resistance of the chains to uncoiling, while the spring represents vibration of chain segments that will tend to seek the lowest energy arrangement.

The representative experimental curves of creep strain versus creep time of the specimens tested at 35^o C under constant stress of 5MPa are presented in figure 13.

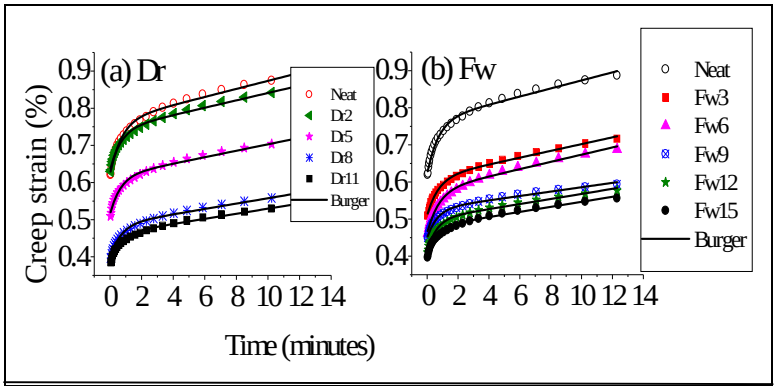

Figure 13: Burger modelling results of the experimental creep data obtained for samples containing various Fiber draws ratios (Dr) (a), and Fiber weight fractions (Fw) (b)

Fittings using Burgers model are drawn in solid lines. It can be seen that the modelling curves show a satisfactory agreement with the experimental data under each condition. The first instantaneous deformation arises from the spring or elastic element (E_M) and later, time-dependent deformation comes from the parallel spring (E_K) and dashpot (η_K) and from the viscous dashpot (η_M). The complete modelling parameters for the SRPPCs are listed in table 2.

According to these results, all the Burger parameters showed an increasing tendency with fiber draw ratio and fiber weight fraction. The general observation is that Dr and Fw composites exhibited higher values of the parameters compared to the neat matrix. These observations strongly suggest that fiber drawing reduce molecular mobility which leads to increased stiffness and hence high resistance to deformation of the SRPPCs.

According to Burger's equation ($\varepsilon_B = \frac{\sigma_o}{E_M} + \frac{\sigma_o}{E_K}\left(1 - e^{\frac{-t\eta_K}{E_K}}\right) + \frac{\sigma_o t}{\eta_M}$), it is shown that the modulus E_M

of the Maxwell spring determined the instantaneous elastic creep strain, which could be immediately recovered on the removal of stress. In general, the composites showed higher E_M values compared to the matrix (neat sample). E_M of each sample category showed an increasing tendency, which can be understood that the bulk materials become rigid and the stiffness is thus increased with the rising modulus. The instantaneous elasticity E_M reasonably corresponds to the elasticity of the crystallized polymer and oriented chains which take the immediate load due to high stiffness compared to the neat matrix. Better elasticity (> 12 MPa) was exhibited by the composites, showing an effective reinforcement by the addition of oriented PP fibers.

Sample category	Specimen	Burger parameters			
		E_M	E_K	η_M	η_K
Neat	Neat	6.15 ± 0.033	34.92 ± 1.43	460.26 ± 32.57	47.87 ± 5.76
Dr	Dr2	7.90 ± 0.045	45.86 ± 1.96	503.79 ± 30.77	66.62 ± 8.31
	Dr5	9.72 ± 0.065	49.19 ± 2.11	575.44 ± 37.27	74.25 ± 9.23
	Dr8	12.60 ± 0.08	56.29 ± 2.18	694.20 ± 43.04	81.83 ± 9.23
	Dr11	12.99 ± 0.08	65.58 ± 2.57	731.33 ± 41.87	91.42 ± 10.5
Fw	Fw3	9.81 ± 0.05	49.63 ± 1.43	547.50 ± 30.04	67.37 ± 7.50
	Fw6	10.82 ± 0.07	43.84 ± 1.71	513.45 ± 31.01	57.00 ± 6.58
	Fw9	11.13 ± 0.06	64.55 ± 2.58	847.23 ± 56.96	99.78 ± 11.48
	Fw12	12.09 ± 0.08	58.09 ± 2.39	733.06 ± 48.09	94.14 ± 11.01
	Fw15	12.54 ± 0.08	62.84 ± 2.52	735.97 ± 45.07	89.86 ± 10.53

Table 2: Parameters of the Burgers model for the SRPPCs

At the molecular level, because of reduced mobility of amorphous chains and even chain folds the stiffness of the bulk material was significantly increased with high E_M.

The retardant elasticity E_K and viscosity η_K of each sample showed a similar dependency on consolidation temperature, consolidation time, fiber draw ratio and fiber weight fraction as E_M (Table 2). It can be described that the deformation of the Kelvin unit of the material decreased with increasing draw ratio (Dr), and fiber weight fraction Fw. The time-dependent E_K and η_K in the Kelvin unit can be associated with the stiffness and viscous or orientation flow of the amorphous polymer chains in short term. The Kelvin unit showed extremely high modulus and very difficult viscous flow, which is enhanced by good interfacial strength, reduced void content at the optimum consolidation temperature and highly oriented fibers. It can be pointed out that fiber draw ratio and fiber weight fraction are most effective to retard the deformation of the Kelvin elements and, especially if optimum consolidation temperature is used.

The permanent viscous flow parameter η_M, which represents the irrecoverable creep, shows a factor of several tens higher than η_K (Table 2). It can be seen that η_M was significantly increased with high Dr and Fw, reflecting the fact of decreasing irrecoverable deformation. The irrecoverable creep strain was decreased by the addition of highly oriented PP fibers, which enhanced the immobility of polymer chains and resulted in high η_M values. Small deformation of the composite can be attributed to crystallized and oriented chains in the drawn fibers which acted as blocking sites to retard or restrict the slippage of the chain segments. The result indicates that the permanent deformation was reduced and the load applied could not activate many polymer segments or damage polymer structure permanently.

Accordingly, the bulk materials behaved with strong recoverable capability which conformed to decreased creep strain (Figures 4 and 8). Therefore, the orientation of polymer chains to a great extent resulted in highly oriented and crystallized bulk material. Thereafter, the advanced creep flow became much difficult and the resulting η_M was high.In conclusion, the Burger's model has provided a constitutive representation of creep deformation, with the modelling parameters showing a detailed structure-to-property relationship of the self-reinforced polypropylene composites.

4.2. Prediction of long-term properties of SRPPCs using Time- temperature superposition principle (TTSP)

One of the greatest constrains in studying the viscoelastic behaviour of polymers is the relatively long time required for performing a test. Hence, methods that are able to predict long-term data have gained considerable attention. Several observations show that the effects of time and temperature are equivalent. The related time-temperature superposition principle is one of the most widely used extrapolation technique that has been applied to virtually every mechanical property and each kind of plastic. TTSP implies that the viscoelastic behaviour at one temperature (T_{ref}) can be related to that at another temperature by a shift, a_T, in time-scale only (6) [26-28].

$$\dot{t} = \frac{t}{a_T} \quad (6)$$

where $\dot{t}$ is the shifted, or reduced, time; t is the elapsed time of a test and $a_T$is the shift factor specific to a test.

For any reference temperature chosen, a fully overlapped continuous curve called a master curve is formed. This master curve can be used to predict the viscoelastic performance over long time scale. The master curve can also be used to determine the time at which a particular viscoelastic quantity reaches some critical value. TTSP can be used to obtain the master curves for several properties such as creep, creep compliance, and stress compliance versus time (or log (t)) or dynamic modulus against frequency [29-32].

The shift factor is usually described either by the Williams-Landel-Ferry (WLF) equation or the Arrhenius relationship. The WLF equation, is described as

$$\log a_T = -\frac{C_1(T - T_o)}{C_2 + (T - T_o)} \quad (7)$$

whereC_1 and C_2 are constants dependent on the nature of the material, T is the test temperature and T_o is the reference temperature (C1=17.4 and C2=51.6°K if, $T_o = T_g$).

The use of WLF equation is restricted to materials above the glass transition temperature [32] or in the glass transition region [33]. The equation is based on the assumption that, above the glass transition temperature, the fractional free volume increases linearly with respect to temperature. The model also assumes that as the free volume of the material increases, its viscosity rapidly decreases [33].

However, some materials do not display a glass transition, but remain crystalline at all temperatures. The relationship between the temperature and the horizontal shift factor, log (a_T), for materials that do not display glass transition or for those that are being studied below the glass transition temperature is based on the Arrhenius equation:

$$\log a_T = \frac{\Delta E_a}{2.303R}\left(\frac{1}{T} - \frac{1}{T_o}\right) \quad (8)$$

where$R$ is the universal gas constant and ΔE_a is the activation energy, and can be obtained from the slope of the curve of log a_T against 1/T. It is fairly believed that TTSP manifests itself from the molecular behaviour and, therefore, equations based on the activation energy, such as the Arrhenius equations are proposed [27].

In the current investigation, short – term (12 minutes) creep experiments of SRPPCs were carried out on the Dr and Fw sample categories at five different temperatures (30, 45, 60, 75, 90^{o}C). The creep data were then shifted horizontally along the logarithmic time axis until they overlapped to form one continuous master curve, which could be used to predict creep performance over long time scale. For all the master curves, the reference temperature was 30^{o}C. Figure 14 shows the creep master curves obtained. The master curves show resistance to creep by both sample categories as expected. However, the Fw15 and Dr11 samples exhibit higher intensity resistance to creep deformation. This difference in creep behaviour between the various categories can be explained by the resulting composite morphology, as discussed in the sections before, and also indicates that the characteristics of the reinforcement and the processing conditions can significantly affect the long-term viscoelastic behaviour of the self-reinforced PP composites. From the master curves, the creep behaviour of the composite could be traced over an extended time scale of order 10^8 minutes that is much wider than that determined experimentally.Shift factors, a_T were obtained directly from the experimental creep curves plotted against time by measuring the amount of shift along the time scale necessary to superimpose the curves on the reference.

The reference temperature was taken as 30^{o}C for all the creep curves irrespective of the sample category or type. The log a_T values thus, obtained by shifting at different temperatures are listed in Table 3. They show that the absolute value of log a_T increases with increasing temperature, it decreases with increasing fiber weight fraction and increases with fiber draw ratio. A higher shift value thus indicates a larger shift of the creep curve to the reference curve. The negative sign implies that shifting was towards the right.

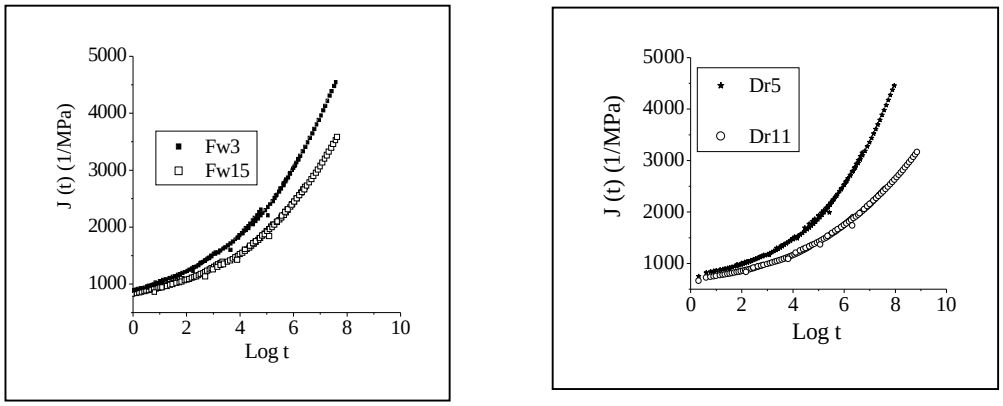

Figure 14: Creep master curves for various sample categories of SRPPCs

Temperature (°C)	Log a_T			
	Fw9	Fw 15	Dr5	Dr11
30	0	0	0	0
45	-1.6	-1.3	-1.2	-1.85
60	-3.25	-3.0	-2.75	-3.5
75	-4.4	-4.15	-3.85	-4.75
90	-5.65	-5.35	-5.1	-6.0

Table 3: Shift factors (log a_T) for the SRPPCs

The temperature dependence of the shift factors, a_T was also investigated using the Arrhenius relation $(log a_T = \frac{\Delta E_a}{2.303R})$. When the shift factors were plotted against inverse of temperature (Figure 15), the resultant graphs exhibited a linear relationship. These indicate that the shift data can be best described in terms of the Arrhenius equation. The slope of each graph for the respective sample categories was calculated and used to obtain the activation energies, E_a, using Arrhenius equation.

The list of activation energies calculated is contained in Table 4. Activation energy is observed to increase with Dr, and Fw. Increase in activation energy is in agreement with increase in stiffness, creep resistance, fatigue strength and decomposition temperature.

The higher activation energies also are in good agreement with the effective reinforcing effect of drawn fibers and good fiber/matrix adhesion.

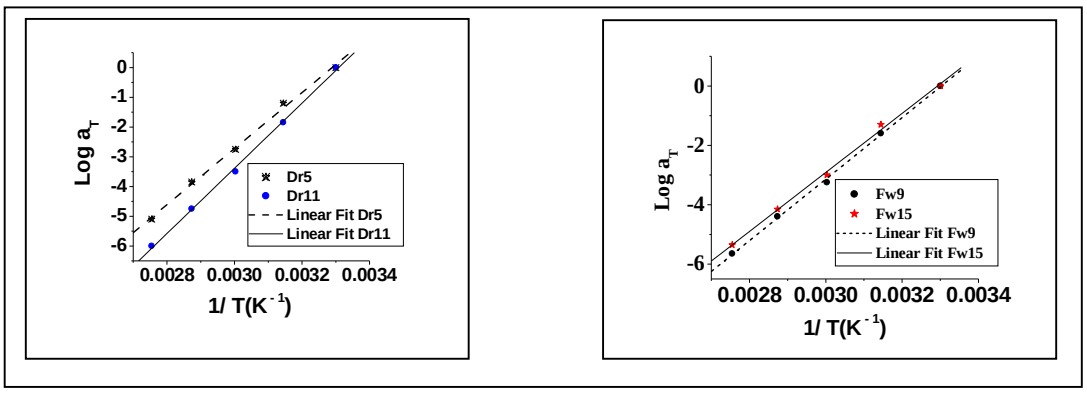

Figure 15: Plots of log a_T versus (1/T) for SRPPCs

	Fw9	**Fw15**	**Dr5**	**Dr11**
Slope (K)	0.093	0.129	0.114	0.127
Ea (kJ/mol)	178.1	247.0	218.3	243.2

Table 4: The activation energy for different sample categories of SRPPCs

5. Conclusions

The goal of this research was to fabricate SRPPCs using PP fibers of various draw ratios and investigate the effects of fiber draw ratio and fiber weight fraction on dynamic mechanical properties, fatigue, and the creep behaviour of SRPPCs. Based on the results it can be seen that the fiber characteristics and fiber weight fraction determine the quality of mechanical properties of SRPPCs. Consequently the following conclusions can be made:

The composites generally showed an improvement in dynamical properties, fatigue resistance and fatigue life was significantly improved compared to the neat PP matrix. An increase of up to 33% in stiffness was registered in the composite over neat PP matrix.

It was observed that stiffness, creep resistance, and fatigue resistance improved with fiber draw ratio and fiber weight fraction. This was attributed to increased crystallinity in the drawn fibers.

Burgers modelling parameters showed an explicit dependence on fiber characteristics. This indicated the reinforcing effectiveness of the drawn PP fibers on the SRPPCs and suggested the structure-property relationship.

6.References

1. 2000/53/EC, Directive 2000/53/EC of European Parliament and of the Council of 18 September 2000 on End-of-Life Vehicles; (2000).
2. Izer A., Bárány T., Varga J.: Development of woven fabric reinforced all-polypropylene composites with beta nucleated homo- and copolymer matrices. Composites Science and Technology, 69, 2185–2192 (2009).
3. DOI: 10.1016/j.compscitech.2009.06.002
4. Alcock B., Cabrera N. O., Barkoula N-M., Reynolds C. T., Govaert L. E., Peijs T.: The effect of temperature and strain rate on the mechanical properties of highly oriented polypropylene tapes and all-polypropylene composites. Composites Science and Technology, 67, 2061–2070 (2007).
5. DOI: 10.1016/j.compscitech.2006.11.012
6. Bhattacharyya D., Maitrot P., Fakirov S.: Polyamide 6 single polymer composites. Express Polymer Letters, 3, 525–532 (2009).
7. DOI: 10.3144/expresspolymlett.2009.65
8. Alcock B., Cabrera N. O., Barkoula N. M., Loos J., Peijs T.: The mechanical properties of unidirectional all-polypropylene composites. Composites Part A: Applied Science and Manufacturing, 37, 716–726 (2006).
9. DOI: 10.1016/j.compositesa.2005.07.002
10. 6. Alcock B., Cabrera N. O., Barkoula N-M., Spoelstra A. B., Loos J., Peijs T.: The mechanical properties of woven tape all-polypropylene composites. Composites Part A: Applied Science and Manufacturing, 38, 147–161 (2007).
11. DOI: 10.1016/j.compositesa.2006.01.003
12. 7. Bárány T., Izer A., Karger-Kocsis J.: Impact resistance of all-polypropylene composites composed of alpha and beta modifications. Polymer Testing, 28, 176–182 (2009).
13. DOI: 10.1016/j.polymertesting.2008.11.011
14. 8. Houshyar S., Shanks R. A.: Mechanical and thermal properties of toughened polypropylene composites. Journal of Applied Polymer Science, 105, 390–397 (2007).
15. DOI: 10.1002/app.25034
16. 9. Houshyar S., Shanks R. A., Hodzic A.: Tensile creep behaviour of polypropylene fibre reinforced polypropylene composites. Polymer Testing, 24, 257–264 (2005).
17. DOI:10.1016/j.polymertesting.2004.07.003
18. 10. Greco A., Musardo C., Maffezzoli A.: Flexural creep behaviour of PP matrix woven composite. Composites Science and Technology, 67, 1148–1158 (2007).
19. DOI: 10.1016/j.compscitech.2006.05.015
20. 11 .Acha B. A., Reboredo M. M., Marcovich N. E.: Creep and dynamic mechanical behavior of PP-jute composites: Effect of the interfacial adhesion. Composites Part A: Applied Science and Manufacturing, 38, 1507–1516 (2007).
21. DOI: 10.1016/j.compositesa.2007.01.003
22. 12 .Kim K. J., Yu W-R., Harrison P.: Optimum consolidation of self-reinforced polypropylene composite and its time-dependent deformation behavior. Composites Part A: Applied Science and Manufacturing, 39, 1597–1605 (2008).
23. DOI: 10.1016/j.compositesa.2008.06.005
24. 13. Chartoff R. P.: Thermoanalytical instrumentation, techniques and methodology. inThermoplastic Polymers (ed.: Turi E. A.) Academic Press, San Diego, 483–743 (1997).
25. 14 .Alcock B., Cabrera N. O., Barkoula N. M., Wang Z., and Peijs T. (2008): The effect of temperature and strain rate on the impact performance of recyclable all-polypropylene composites. Composites Part B: Engineering, 39, 537-547.
26. 15 .Alcock B., Cabrera N. O., Barkoula N. M., and Peijs T. (2006): Low velocity impact performance of recyclable all-polypropylene composites. Composite Science and Technology 66, 1724-1737 (2006).
27. 16 .Reading. M., Haines. P.J.; Thermomechanical, dynamic mechanical and associated methods in; P. J. Haines; Thermal methods of analysis: Principles, Applications and Problems Blackie, London pp.123-160 (1995).
28. 17 .Acha, B., Reboredo, M., and Marcovich, E.: Creep and dynamic mechanical behaviour of PP-jute composites: Effect of the interfacial adhesion. Composites Part A-Applied Science and Manufacturing, 38, 1507-1516 (2007).
29. 18 .Hevin P. M,: Dynamic mechanical analysis: A practical Introduction. CRC Press, Taylor and Francis Group, Boca Raton, London New York (2008).

30. 19 .Findley, W. N., Lai, J. S., Onaran, K.,: Creep and relaxation of nonlinear viscoelastic materials: with an introduction to linear viscoelasticity. Dover Publications Inc. New York (1989).
31. 20 .Ward I. M. and Hadley D. W.: An Introduction to the Mechanical Properties of Solid Polymers, Wiley, New York (1993).
32. 21 .Pegoretti, A., Zanolli, A., and Migliaresi, C.: Preparation and tensile mechanical properties of unidirectional liquid crystalline single polymer composites. Composites Science and Technology, 66, 1970–1979 (2006).
33. 22 .Tschoegl, N.: The phenomenological theory of linear viscoelasticity, Springer-Verlag, Berlin Germany (1989).
34. 23 .Marcovich, N. E., and Villar, M. A.: Thermal and mechanical characterization of linear low density polyethylene/wood flour composites. Journal of Applied Polymer Science, 90, 2775-2784 (2003).
35. 24 .Peng, K., Jia, Y., Xing-Long, G.,Zhong, Z.: Creep and recovery of polypropylene/carbon nanotube composites. International Journal of Plasticity, 10, 1016 (2011).
36. 25 .Banik K., Karger-Kocsis J., Abraham T.: Flexural creep of all-polypropylene composites: Model analysis. Polymer Engineering and Science, 48, 941–948 (2008).
37. DOI: 10.1002/pen.21041
38. 26 .Ward, I. M.: Mechanical Properties of Solid Polymers. John Wiley and Sons Ltd., Weinheim (1983).
39. 27 .Banik K., Abraham T. N., Karger-Kocsis J.: Flexural creep behavior of unidirectional and cross-ply allpoly(propylene) (PURE®) composites. Macromolecular Materials and Engineering, 292, 1280–1288 (2007).
40. DOI: 10.1002/mame.200700180
41. 28 .William, M. L., Landel, R. F., Ferry, J. D.: The temperature dependence of relaxation mechanisms in amorphous polymers and other glass-forming liquids. Journal of America Chemical Society, 77, 3701-3707 (1955).
42. 29 .Fung, Y. C.: Stress Strain History Relations of Soft Tissues in Simple Elongation, in Biomechanics, its Foundations and Objectives, ed. Fung, Y. C., Perrone, N. and Anliker, M., Prentice Hall, Englewood Cliffs, NJ. (1972).
43. 30 .Lai, J., Bakker A.: Creep and Relaxation of Nonlinear Viscoelastic Materials, Polymer Engineering Science, 35,1339-1347 (1995).
44. 31 .Rowe, G.M., Sharrock M.J., Bouldin M.G., Dongré, R.N.: Advanced Techniques to Develop Asphalt Master Curves from the Bending Beam Rheometer, Petroleum and Coal, 43, 54-59 (2003).
45. 32 .Alwis, K. G. N. C., Burgoyne C. J.: Time-Temperature Superposition to determine the Stress-Rupture of Aramid Fibres, Preprint, University of Cambridge, United Kingdom (2006).
46. 33 .Ferry,J.D.: Viscoelastic Properties of Polymers, 3rd ed. Wiley, New York, (1980).